Ultrasonic transducers: From analytical modelling to design optimisation and validation

Álvaro Pérez Díaz, *Centre for Complexity Science, University of Warwick*
Supervisor: Dr Nishal Ramadas, *Department of Physics, University of Warwick*
Co-supervisor: Dr Gareth Alexander, *Centre for Complexity Science, University of Warwick*

***Abstract*—The most important part in an ultrasonic transducer is a piezoelectric substrate, which will accumulate electric charge in response to an applied mechanical stress. In the most typical configuration, one layer of such a piezoelectric material will be present altogether with some passive backing and matching layers, situated in the back and in the front of the transducer, respectively.**

Complexity in ultrasonic transducers design has increased in the last decades: even with the most simple configuration there is a huge variety of possible designs: backing layers, matching layers, electrical load, piezoelectric elements, etc. All this makes intuitive design very difficult. When it comes to model this kind of device, there are three different choices: Finite Element (FE), equivalent circuit or analytical models. The latter provide physical insight into the processes taking place in the transducer, as well as being fast and suited for optimization purposes.

We will have a look at two typical analytical models available in literature, afterwards we shall consider a third one, which has to be modified to fit our purposes. Then some comparisons will be performed among the three analytical models, real laboratory data, and a FE commercial software.

I. INTRODUCTION

We will start by considering the physics behind piezoelectric and non-piezoelectric materials, having a look at their governing equations and including some assumptions that will let us derive our models. All the above altogether with some technical details that will constitute the framework for the first two models will shape section 2. [1], [2], [3].

In the third and fourth sections we describe and analyze the models given in [2]-[5] respectively. The first one is the simplest model and will provide clear distinction between receiving and transmitting modes, as well as being a very good introduction to more complicated setups. The second one introduces arbitrary layer possibilities providing better behaviour.

Section 4 introduces a model based on [6] that uses a slightly different framework than the previous two ones, all the required tools will be detailed there. Originally it considered a different setup which is of no use for us, so we had to modify and redo the calculations to fit our purposes.

To finish, several results and experiments are described, providing evidence of the capabilities that this analytical models have when it comes to model real world ultrasonic transducers.

Symbol list

- ξ, *particle displacement* (m)
- S, *area* (m^2)
- F, *force,* (N)
- $\Gamma = F/S$, *stress* (N/m^2)
- $\partial\xi/\partial x$, *strain*
- Y, *elastic constant under conditions of constant electrical displacement* (N/m^2)
- ρ, *density* (kg/m^3)
- h, *piezoelectric constant* (V/m)
- E, *electric field* (V/m)
- D, *electrical displacement* (C/m^2)
- ε, *permittivity under conditions of constant strain* (F/m)
- s, *Laplace complex variable*

II. GOVERNING EQUATIONS

We shall distinguish two different kinds of materials, depending on whether they are piezoelectrically active or not:

- For non-piezoelectric materials: the two equations governing their behaviour are

$$\begin{cases} \Gamma = Y\dfrac{\partial\xi}{\partial x} & \text{(1a)} \\ \rho\dfrac{\partial^2\xi}{\partial t^2} = \dfrac{\partial\Gamma}{\partial x} & \text{(1b)} \end{cases}$$

  where (1a) is Hooke's law between stress and strain, and (1b) is second Newton's law for an infinitesimal volume element.
  If we now combine both equations after taking partial derivative with respect to x in (1a):

$$\frac{\partial\Gamma}{\partial x} = Y\frac{\partial^2\xi}{\partial x^2} \Longrightarrow \rho\frac{\partial^2\xi}{\partial t^2} = Y\frac{\partial^2\xi}{\partial x^2} \Longrightarrow \frac{\partial^2\xi}{\partial t^2} = v^2\frac{\partial^2\xi}{\partial x^2}$$

  where $v^2 = \dfrac{Y}{\rho}$. This is the equation waves travelling in this non-piezoelectric material must satisfy.
- For piezoelectric materials: the equations are similar but in this case we have to include the piezoelectric behaviour of the material, represented by its piezoelectric constant h, obtaining the set of equations:

$$\begin{cases} \Gamma = Y\dfrac{\partial\xi}{\partial x} - hD & \text{(2a)} \\ E = -h\dfrac{\partial\xi}{\partial x} + D/\varepsilon & \text{(2b)} \\ \rho\dfrac{\partial^2\xi}{\partial t^2} = \dfrac{\partial\Gamma}{\partial x} & \text{(2c)} \end{cases}$$

again, if we take partial derivative of (2a) with respect to x and combine it with (2c), we get

$$\frac{\partial \Gamma}{\partial x} = Y \frac{\partial^2 \xi}{\partial x^2} - h \frac{\partial D}{\partial x} \Longrightarrow \frac{\partial^2 \xi}{\partial t^2} = \frac{Y}{\rho} \frac{\partial^2 \xi}{\partial x^2} - \frac{h}{\rho} \frac{\partial D}{\partial x}$$

If we are considering a thickness mode, this is, we assume the transducer to vibrate predominantly in one dimension (thickness dimension), we can perform the following derivation:

$$\frac{\partial D}{\partial y} = \frac{\partial D}{\partial z} = 0$$

and using Gauss' law together with the fact that there is no free charge inside the transducer (all the possible charge would be located at the electrodes) yields to

$$\nabla \cdot \mathbf{D} = \rho_{\text{inside}} = 0 \Longrightarrow \frac{\partial D}{\partial x} = 0$$

hence in our previous equation we can get rid of the last term:

$$\frac{\partial^2 \xi}{\partial t^2} = \frac{Y}{\rho} \frac{\partial^2 \xi}{\partial x^2} \text{ , where } v^2 = \frac{Y}{\rho} \tag{3}$$

which is an identical wave equation to the one obtained for non-piezoelectric materials.

To solve the wave equation it is useful to use the Laplace transform, together with the assumption that all functions are zero at $t = 0$

$$\mathcal{L}[f(t)] = \overline{f}(t) = \int_0^\infty e^{-st} f(t) dt$$

we shall apply it to our wave equation to obtain

$$\frac{s^2}{v^2} \overline{\xi}(s,x) = \frac{\partial^2 \overline{\xi}(s,x)}{\partial x^2}$$

and its general solution will be

$$\overline{\xi}(s,x) = A e^{-sx/v} + B e^{sx/v} \text{ , } A, B \in \mathbb{R}$$

From now on, for the rest of this chapter and in the two following ones, we shall use Laplace transformed functions, even if we omit the over line sign in some functions for the sake of clarity.

We can now relate the total force exerted over an area S normal to the x direction, $F = \Gamma S$

- For a non-piezolectric material, using (1a)

$$\Gamma = \frac{F}{S} = \frac{s}{v} Y \left[-A e^{-sx/v} + B e^{sx/v} \right] \Longrightarrow$$

$$\Longrightarrow F = Z s \left[-A e^{-sx/v} + B e^{sx/v} \right] \tag{4}$$

where $Z = \rho v S$ is the *characteristic acoustic impedance* of the material (note that in some texts the cross sectional area S is omitted).

- For a piezoelectric material, using (2a)

$$\Gamma = Y \frac{s}{v} \left[-A e^{-sx/v} + B e^{sx/v} \right] - hD$$

and applying again Gauss' law to the surface of the piezoelectric material (in our case, where the electrodes are located, this is front and rear faces)

$$\int_S \mathbf{D} \cdot d\mathbf{s} = DS = \int_V \rho_{\text{charge}} = Q \Longrightarrow \frac{Q}{S} = D$$

combining this results we obtain

$$F + hQ = s Z_c \left[-A e^{-sx/v} + B e^{sx/v} \right]$$

We can also find the voltage across the piezoelectric transducer by integrating (2b) from $x = 0$ to $x = L$ (all the thickness of the transducer):

$$V = \int_0^L E dx = \int_0^L \left[-h \frac{\xi}{\partial x} + \frac{D}{\varepsilon} \right] dx =$$

$$= -h \left[\xi(L) - \xi(0) \right] + \frac{Q}{C_0}$$

F where $C_0 = S\varepsilon / L$ is the *clamped* or *static capacitance* of the transducer. We can rewrite our expression as follows

$$V = -h \left[\xi(L) - \xi(0) \right] \overline{U} \text{ , where } \overline{U} = \frac{s C_0 Z_e}{1 + s C_0 Z_e}$$

being Z_e the impedance of an arbitrary electrical load connected across the transducer electrodes.

Note that if we had multiple piezoelectric layers, the overall voltage across the whole transducer would be the sum of the correspondent voltages for each of the layers

$$V = \int_{a_1}^{b_1} E_1 dx + \ldots + \int_{a_n}^{b_n} E_n dx$$

III. Linear Systems Model (LSM)

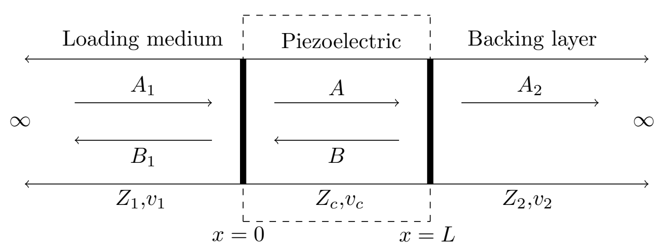

Fig. 1: Basic setup for a transducer with an infinite backing layer (at $x = 0$) and in contact with a loading medium at its front face ($x = L$).

The boundary conditions that apply for the wave equation solution are: continuity of particle displacements, ξ and continuity of forces across the interface, F, at the front and rear face, resulting in four boundary equations:

$$\begin{cases} \xi_{1_{|x=0}} = \xi_{c_{|x=0}} \\ \xi_{c_{|x=L}} = \xi_{2_{|x=L}} \\ F_{1_{|x=0}} = F_{c_{|x=0}} \\ F_{c_{|x=L}} = F_{2_{|x=L}} \end{cases}$$

where each of the expressions has the following form:

$$\begin{cases} \xi_1(s) = A_1 e^{-sx/v_1} + B_1 e^{sx/v_1} \\ \xi_c(s) = A e^{-sx/v_c} + B e^{sx/v_c} \\ \xi_2(s) = A_2 e^{-sx/v_2} \end{cases}$$

$$\& \quad \begin{cases} F_1(s) = sZ_1\left(-A_1 e^{-sx/v_1} + B_1 e^{sx/v_1}\right) \\ F_c(s) + hQ(s) = sZ_c\left(-Ae^{-sx/v_c} + Be^{sx/v_c}\right) \\ F_2(s) = sZ_2\left(-A_2 e^{-sx/v_2}\right) \end{cases}$$

hence the resulting equations are:

$$\begin{cases} A_1 + B_1 = A + B & \text{(5a)} \\ Ae^{-sL/v_c} + Be^{sL/v_c} = A_2 e^{-sL/v_2} & \text{(5b)} \\ sZ_1\left(-A_1 + B_1\right) = sZ_c(-A+B) - hQ(s) & \text{(5c)} \\ sZ_c\left(-Ae^{-sL/v_c} + Be^{sL/v_c}\right) = \\ \quad = sZ_2\left(-A_2 e^{-sL/v_2}\right) - hQ(s) & \text{(5d)} \end{cases}$$

altogether with the expression for the voltage

$$V = -h\left[A(e^{-sL/v_c} - 1) + B(e^{sL/v_c} - 1)\right]\overline{U}(s) \tag{6}$$

Now, combining (5a) and (5c) we obtain

$$(1 - R_F)A_1 = A - BR_F + \frac{hQ(s)}{s(Z_c + Z_1)} \tag{7}$$

$$\text{where } R_F = \frac{Z_c - Z_1}{Z_c + Z_1}$$

and similarly from (5b) and (5d)

$$Ae^{-2sL/v_c}R_B - B = -\frac{hQ(s)e^{sL/v_c}}{s(Z_2 + Z_c)} \tag{8}$$

$$\text{where } R_B = \frac{Z_c - Z_2}{Z_c + Z_2}$$

Both R_F and R_B are the reflection coefficients for the waves travelling *into* the piezoelectric medium.

Now combine equations (7) and (8) and solve for A and B, using for example Cramer's rule, to obtain:

$$A = \frac{\left\{\dfrac{hQ(s)}{s(Z_c + Z_1)} + (R_F - 1)A_1 - \dfrac{hQ(s)R_F e^{-sL/v_c}}{s(Z_2 + Z_c)}\right\}}{\left\{e^{-2sL/v_c}R_B R_F - 1\right\}} \tag{9}$$

$$B = \frac{\begin{array}{l} -\dfrac{hQ(s)e^{-sL/v_c}}{s(Z_c + Z_2)} - (1 - R_F)A_1 R_B e^{-2sL/v_c} + \\ \qquad + \dfrac{hQ(s)R_B e^{-2sL/v_c}}{s(Z_c + Z_1)} \end{array}}{\left\{e^{-2sL/v_c}R_B R_F - 1\right\}} \tag{10}$$

We can now find the voltage across the transducer, plugging (9) and (10) into (6) to obtain

$$V = h\left\{K_F\left[A_1(1 - R_F) - \frac{hQ}{s(Z_c + Z_1)}\right] - K_B\frac{hQ}{s(Z_c + Z_2)}\right\} \tag{11}$$

We shall now develop the receiver and transmitter models, using the framework just detailed. This has the advantage of showing very clearly both functioning modes, which are quite independent from each other.

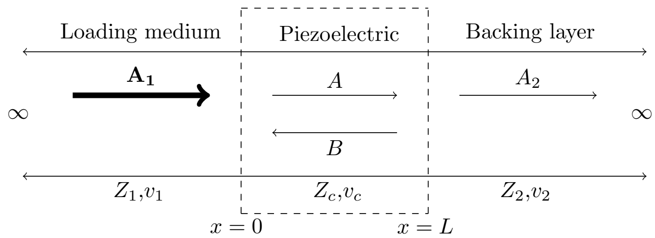

Fig. 2: Basic setup for a transducer in recevier mode with an infinite backing layer (at $x = 0$) and in contact with a loading medium at its front face ($x = L$)

A. Receiver mode

In receiver mode, there is no emitterd left going wave, we will just consider the incident wave (A_1).

Remember the equation for the force (4), together with the previous assumptions:

$$F_1 = Z_1 s\left[-A_1 e^{-sx/v_1} + B_1 e^{sx/v_1}\right] \Longrightarrow$$
$$\Longrightarrow F_1 = -A_1 Z_1 s \Longrightarrow A_1 = -\frac{-F_1}{Z_1 s}$$

Also replace $Q = -V/sZ_e$, which follows from Ohm's law $Z = V/I$, to obtain for the voltage

$$V = \frac{hA_1 K_F(1 - R_F)U(s)}{1 - h^2\left[\dfrac{K_F}{Z_c + Z_1} + \dfrac{K_B}{Z_c + Z_2}\right]\dfrac{U(s)}{s^2 Z_e}}$$

and substituting $A_1 = -\dfrac{-F_1}{Z_1 s}$ yields to:

$$\boxed{\frac{V}{F_1} = \frac{-hK_F T_F U(s)/sZ_c}{1 - h^2\left[\dfrac{K_F T_F}{2} + \dfrac{K_B T_B}{2}\right]\dfrac{U(s)}{s^2 Z_e Z_c}}} \tag{12}$$

which is the transfer function relating the transforms of received voltage to incident force.

We can represent this transfer function using a block diagram with two positive feedback loops, see figure 3.

If we replace R_B by R_F and vice versa, we obtain a transfer function for the force applied in the rear face of the transducer. However, as we assume a infinitely long backing block and hence no returning wave, there will not be any rear face applied force.

B. Transmitter mode

This is an analogous situation, where now there is no incident wave (see figure 4). Setting $A_1 = 0$ into (11) yields to

$$A = \frac{\dfrac{hQT_F}{2Z_c s} - \dfrac{hQT_B R_F e^{-sL/v_c}}{2sZ_c}}{e^{-2sL/v_c}R_B R_F - 1}$$

$$B = \frac{-\dfrac{hQT_B e^{-sL/v_c}}{2sZ_c)} + \dfrac{hQT_F R_B e^{-2sL/v_c}}{2sZ_c)}}{e^{-2sL/v_c}R_B R_F - 1}$$

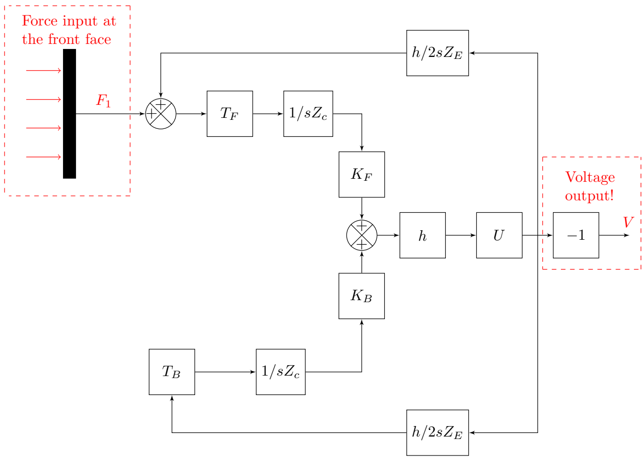

Fig. 3: Receiver transfer function

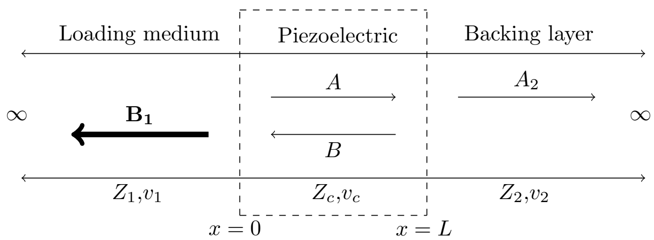

Fig. 4: Basic setup for a transducer in transmit mode with an infinite backing layer (at $x = 0$) and in contact with a loading medium at its front face ($x = L$)

which plugged into (6) result in

$$V = \frac{Q}{C_o}\left[1 - \frac{h^2 C_o}{2sZ_c}\left(T_F K_F + T_B K_B\right)\right] \tag{13}$$

From this expression we can determine the *operational impedance* of the transducer, Z_T:

$$\boxed{Z_T = \frac{V(s)}{sQ(s)} = \frac{1}{sC_o}\left[1 - \frac{h^2 C_o}{2sZ_c}(T_F K_F + T_B K_B)\right]} \tag{14}$$

The next step is to find the force at any point within the transducer. Recall the expression for the force in a piezoelectric layer

$$F_c(s) + hQ(s) = sZ_c\left(-Ae^{-sx/v_c} + Be^{sx/v_c}\right)$$

and using our values for A and B:

$$\begin{aligned} F(s) = &- hQ(s)\left\{1 + \frac{1}{2s(e^{-2sL/v_c}R_B R_F - 1)}\cdot\right. \\ &\cdot\left[(T_F - T_B R_F e^{-sL/v_c})e^{-sx/v_c} + \right. \\ &\left.\left. +(T_B e^{-sL/v_c} - T_F R_B e^{-2sL/v_c})e^{sx/v_c}\right]\right\} \end{aligned}$$

We are now particularly interested in the front and back faces of the transducer. Thus, set $x = 0$ and $x = L$ respectively:

$$F_F(s) = F_{|x=0} = -hQ(s)K_F\frac{Z_1}{Z_c + Z_1} \tag{15}$$

$$F_B(s) = F_{|x=L} = -hQ(s)K_B\frac{Z_2}{Z_c + Z_2} \tag{16}$$

The final step will be, as we did for the receiver mode, to find a transfer function relating the force generated at the front face to the voltage across the transducer. Notice that we have obtained forces in both rear and front faces, but we are primarily interested in the front face.

Consider the following electrical setup:

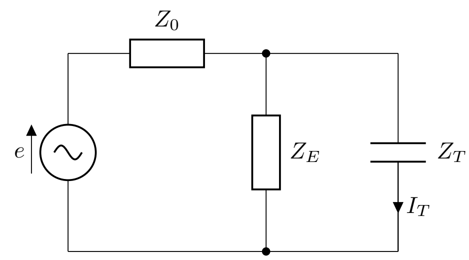

Fig. 5: Circuit schematics for the transmitter mode

where Z_o is the output impedance of the non-ideal voltage source used, and Z_E is an arbitrary electrical load. Using circuit analysis we obtain the following relation:

$$\begin{aligned} \frac{I_T(s)}{e(s)} &= \frac{Z_E}{Z_T(Z_o + Z_E) + Z_o Z_E} = \frac{Z_E/(Zo + Z_e)}{Z_T + Z_o Z_E/(Z_o + Z_E)} = \\ &= \frac{a(s)}{Z_T + b(s)} \Longrightarrow I_T(s) = \frac{a(s)e(s)}{Z_T + b(s)} \Longrightarrow \\ &\Longrightarrow Q = \frac{I_T(s)}{s} = \frac{a(s)e(s)}{Z_T + b(s)} \end{aligned}$$

where

$$a(s) = \frac{Z_E}{Z_o + Z_E} \quad \& \quad b(s) = \frac{Z_o Z_E}{Z_o + Z_E}$$

We can now use the new expression for $Q(s)$ and (14) into (15) to obtain

$$\boxed{\frac{F_F(s)}{e(s)} = -\frac{h\, a(s)Z_1/(Z_c + Z_1)K_F(s)Y(s)}{1 - h^2 Y(s)/(sZ_c)\,\left(T_F K_F/2 + T_B K_B/2\right)}} \tag{17}$$

which is the desired transfer equation, with $Y(s) = (1 + sb(s)C_o)/C_o$.

In a completely similar fashion we can obtain the transfer function for the back face:

$$\boxed{\frac{F_B(s)}{e(s)} = -\frac{h\, a(s)Z_2/(Z_c + Z_2)K_B(s)Y(s)}{1 - h^2 Y(s)/(sZ_c)\,\left(T_F K_F/2 + T_B K_B/2\right)}} \tag{18}$$

This transfer function can be pictured again in a block diagram structure, see figure 6.

IV. Lattice Model

CONSIDER the setup outlined in figure 7, where medium 2, with a thickness l_2, is located between media 1 and 3, which are semi-infinite. We decompose forces into their backward B_n and frontward F_n components. The

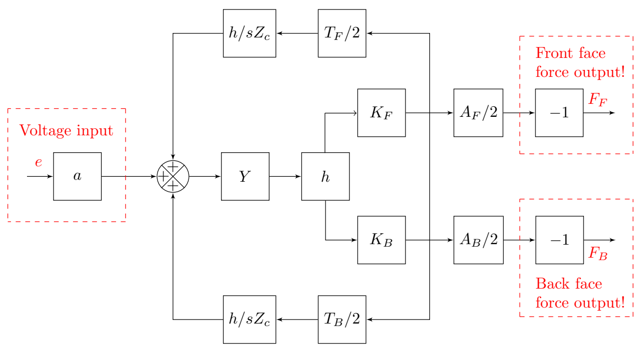

Fig. 6: Transmitter transfer function

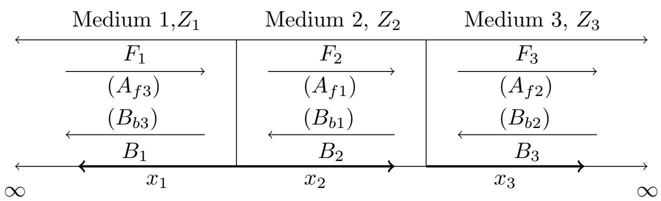

Fig. 7: Basic setup for a number of passive layers. Displacements are bracketed.

same for the displacements, backward B_{bn} and frontward A_{an}.

Again, using complex Laplace transforms and the same analysis as for the systems model, we obtain:

$$\begin{cases} \overline{\xi}_n = \overline{A}_{fn} e^{-sx_n/v_n} + \overline{B}_{bn} e^{sx_n/v_n} & (19a) \\ \overline{\Gamma}_n = sZ_n[-\overline{A}_{fn} e^{-sx_n/v_n} + \overline{B}_{bn} e^{sx_n/v_n}] & (19b) \end{cases}$$

Define now the force components at position x_n to be

$$\overline{F}_n = -sZ_n\overline{A}_{fn} \;\;\&\;\; \overline{B}_n = sZ_n\overline{B}_{bn}$$

so we can rewrite (19a) and (19b) as

$$\begin{cases} \overline{\xi}_n = [\overline{F}_n e^{-sx_n/v_n} + \overline{B}_n e^{sx_n/v_n}]/sZ_n] & (20a) \\ \overline{\Gamma}_n = \overline{F}_n e^{-sx_n/v_n} + \overline{B}_n e^{sx_n/v_n} & (20b) \end{cases}$$

We shall drop the over lines to make notation clear, recall that for this model everything is done in complex Laplace domain. Consider now the boundaries $x_n = 0$ and $x_n = l_n$ of this n-th layer:

$$F_{n0} = F_n e^{-sx_n/v_n}_{|x_n=0} \;\;\&\;\; B_{n0} = B_n e^{sx_n/v_n}_{|x_n=0}$$

$$F_{nl_n} = F_n e^{-sx_n/v_n}_{|x_n=l_n} \;\;\&\;\; B_{nl_n} = B_n e^{sx_n/v_n}_{|x_n=l_n}$$

hence we can write for the model in the figure

$$\begin{pmatrix} F_{2l_2} \\ B_{2l_2} \end{pmatrix} = \begin{pmatrix} e^{-sT_2} & 0 \\ 0 & e^{sT_2} \end{pmatrix} \begin{pmatrix} F_{20} \\ B_{20} \end{pmatrix}$$

where $T_2 = l_2/v_2$ is the transit time for waves travelling across the layer.

The boundary conditions result as follows

$$\begin{cases} (-F_{10} + B_{10})/Z_1 = (-F_{20} + B_{20})/Z_2 \\ (-F_{2l_2} + B_{2l_2})/Z_2 = (-F_{30} + B_{30})/Z_3 \\ F_{10} + B_{10} = F_{20} + B_{20} \\ F_{2l_2} + B_{2l_2} = F_{30} + B_{30} \end{cases}$$

the the first and the second coming from (20a) and the last two ones from (20b). This can be written in matrix form:

$$\begin{pmatrix} F_{20} \\ B_{10} \end{pmatrix} = \begin{pmatrix} 1 + R_{12} & -R_{12} \\ R_{12} & 1 - R_{12} \end{pmatrix} \begin{pmatrix} F_{10} \\ B_{20} \end{pmatrix}$$

$$\begin{pmatrix} F_{30} \\ B_{2l_2} \end{pmatrix} = \begin{pmatrix} 1 + R_{23} & -R_{13} \\ R_{13} & 1 - R_{13} \end{pmatrix} \begin{pmatrix} F_{2l_2} \\ B_{30} \end{pmatrix}$$

where

$$R_{12} = \frac{Z_2 - Z_1}{Z_2 + Z_1} \;\;\&\;\; R_{23} = \frac{Z_3 - Z_2}{Z_3 + Z_2}$$

are the reflection coefficients for waves of force travelling into the piezo at the 1-2 and 2-3 interfaces respectively.

A. Transducer model

Now consider a similar disposition, placing the piezoelectric layer between two passive layers.

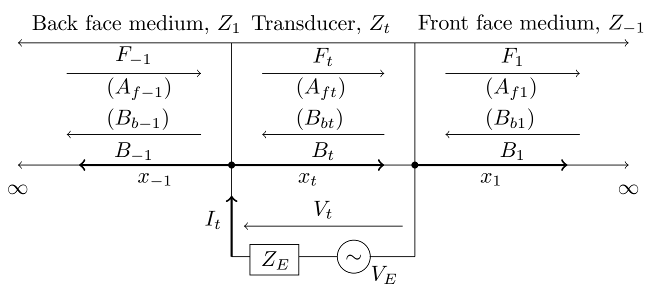

Fig. 8: Piezolectric system. Displacements are bracketed.

The voltage across the transducer will be

$$V_t = -h\left[(\xi_t)_{|x_t=l_t} - (\xi_t)_{|x_t=0}\right] + \frac{Q_t}{C_o} \tag{21}$$

where Q_t is the total electrical charge in the electrodes.

The mechanical boundary conditions are

$$\begin{cases} \xi_{-1|_{x_{-1}=0}} = \xi_{t|_{x_t=0}} \;\;\&\;\; \xi_{t|_{x_t=l_t}} = \xi_{1|_{x_1=0}} \\ \Gamma_{-1|_{x_{-1}=0}} = \Gamma_{t|_{x_t=0}} \;\;\&\;\; \Gamma_{t|_{x_t=l_t}} = \Gamma_{1|_{x_1=0}} \end{cases}$$

that is

$$\begin{cases} (-F_{-10} + B_{-10})/Z_{-1} = (-F_{t0} + B_{t0})/Z_t \\ (-F_{tl_t} + B_{-t_t})/Z_t = (-F_{10} + B_{10})/Z_1 \\ F_{-10} + B_{-10} = F_{t0} + B_{t0} - hQ_t \\ F_{tl_t} + B_{tl_t} - hQ_t = F_{10} + B_{10} - hQ_t \end{cases}$$

$$\& \;\; \begin{pmatrix} F_{tl_t} \\ B_{tl_t} \end{pmatrix} = \begin{pmatrix} e^{-sT_t} & 0 \\ 0 & e^{sT_t} \end{pmatrix} \begin{pmatrix} F_{t0} \\ B_{t0} \end{pmatrix}$$

and in matrix form we obtain

$$\begin{pmatrix} B_{-10} \\ F_{t0} \end{pmatrix} = \begin{pmatrix} R_{-1} & 1 - R_{-1} \\ 1 + R_{-1} & -R_{-1} \end{pmatrix} \begin{pmatrix} F_{-10} \\ B_{t0} \end{pmatrix} + \\ + \frac{h}{2} \begin{pmatrix} R_{-1} - 1 \\ R_{-1} + 1 \end{pmatrix} Q_t \tag{22}$$

$$\begin{pmatrix} F_{10} \\ B_{tl_t} \end{pmatrix} = \begin{pmatrix} R_1 & 1-R_1 \\ 1+R_1 & -R_1 \end{pmatrix} \begin{pmatrix} B_{10} \\ F_{tl_t} \end{pmatrix} + \\ + \frac{h}{2} \begin{pmatrix} R_1 - 1 \\ R_1 + 1 \end{pmatrix} Q_t \tag{23}$$

where

$$R_1 = \frac{Z_t - Z_1}{Z_t + Z_1} \quad \& \quad R_{-1} = \frac{Z_t - Z_{-1}}{Z_t + Z_{-1}}$$

are the usual reflection coefficients for waves of force coming into the piezoelectric medium.

We need to obtain now a relationship between the source voltage and charge, so we can then relate the applied voltage to the one across the transducer. Looking at the electric diagram in figure 8:

$$V_t = V_E - I_t Z_E \quad \text{and} \quad I_t = sQ_t \tag{24}$$

which plugged into (21) gives

$$Q(t) = \frac{C_o}{1 + sC_oZ_E} \left\{ V_E + \frac{h}{sZ_t} \left(1 - e^{-sT_t}\right) \left(F_{t0} + B_{tl_t}\right) \right\} \tag{25}$$

Now using (24) ad (25) we can obtain

$$\frac{V_E - V_t}{sZ_E} = Q_t \Longrightarrow V_t = \frac{V_E}{1 + sC_oZ_E} -$$

$$-\frac{C_o s Z_E}{1 + C_o s Z_E} h(1 - e^{-sT_t})(F_{t0} + B_{tl_t}) \frac{1}{sZ_t} \tag{26}$$

Equations (22), (23) and (26) completely control the behaviour of the transducer: we have three input parameters: F_{-10}, B_{10} and V_E, altogether with three output parameters: F_{10}, B_{-10} and V_t. Then we can develop a transfer function from input to output

$$\begin{pmatrix} F_{10} \\ B_{-10} \\ V_t \end{pmatrix} = (\mathbf{P_{i,j}}) \begin{pmatrix} B_{10} \\ F_{-10} \\ V_e \end{pmatrix}$$

where

$$\mathbf{P} = \begin{pmatrix} P_{11} & P_{12} & P_{13} \\ P_{21} & P_{22} & P_{23} \\ P_{31} & P_{32} & P_{33} \end{pmatrix}$$

The coefficients are found to be

$$\begin{aligned}
P_{11} =& \{(R_1 - R_{-1}e^{-2sT}) + U(1 - e^{-sT})[(e^{-sT} - 1) \cdot \\
& \cdot (1 + R_1R_{-1}) + 2(R_{-1}e^{-sT} - R_1)]\}/P_D \\
P_{12} =& \{(1 - R_1)(1 + R_1)e^{-sT} + U(1 - e^{-sT})(1 + e^{-sT}) \cdot \\
& \cdot (R_1 - 1)(R_{-1} + 1)\}/P_D \\
P_{13} =& G(1 - e^{-sT})(R_1 - 1)(1 - R_{-1}e^{-sT})/P_D \\
P_{21} =& \{(1 - R_{-1})(1 + R_{-1})e^{-sT} + U(1 - e^{-sT}) \cdot \\
& \cdot (1 + e^{-sT})(R_{-1} - 1)(R_1 + 1)\}/P_D \\
P_{22} =& \{(R_{-1} - R_1e^{-2sT}) + U(1 - e^{-sT})[(e^{-sT} - 1) \cdot \\
& \cdot (1 + R_1R_{-1}) + 2(R_1e^{-sT} - R_{-1})]\}/P_D \\
P_{23} =& G(1 - e^{-sT})(R_{-1} - 1)(1 - R_1e^{-sT})/P_D \\
P_{31} =& G(-sZ_E/Z_t)(1 + R_1)(1 - e^{-sT})(1 - R_{-1}e^{-sT})/P_D \\
P_{32} =& G(-sZ_E/Z_t)(1 + R_{-1})(1 - e^{-sT})(1 - R_1e^{-sT})/P_D \\
P_{33} =& \{(1 - R_1R_{-1}e^{-2sT})/(1 + sZ_EC_o) - U(1 - e^{-st}) \cdot \\
& \cdot [(1 + R_1)(1 - R_{-1}e^{-sT}) + (1 + R_{-1})(1 - R_1e^{-sT})] \\
& /P_D\}
\end{aligned}$$

where

$$U = \frac{h^2 C_o}{2sZ_t(1 + sC_oZ_E)} \quad \&$$

$$P_D = \{(1 - R_1R_{-1}e^{-2sT}) - U(1 - e^{-sT})[(1 + R_1) \cdot \\ \cdot (1 - R_{-1}e^{-sT}) + (1 + R_{-1})(1 - R_1e^{-sT})]\}$$

B. The multilayered acoustic lattice

Consider $n+1$ pasive layers as pictured in the figure:

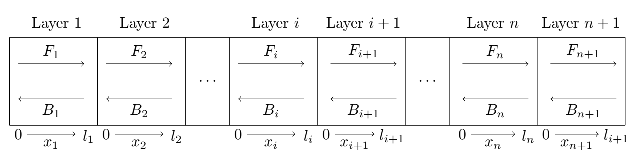

Fig. 9: Pasive multilayer setup, forces F & B.

Consider the interface between layers i & $i+1$, the boundary conditions are

$$\begin{cases} (-F_{il_i} + B_{il_i})/Z_i = (-F_{i+1,0} + B_{i+1,0})/Z_{i+1} \\ F_{il_i} + B_{il_i} = -F_{i+1,0} + B_{i+1,0} \end{cases}$$

hence

$$\begin{cases} -F_{i+1,0} + B_{i+1,0} = Z_{i+1}/Z_i(-F_{il_i} + B_{il_i}) \\ F_{i+1,0} + B_{i+1,0} = F_{il_i} + B_{il_i} \end{cases}$$

if we add and subtract both equations we obtain the following

$$\begin{pmatrix} F_{i+1,0} \\ B_{i+1,0} \end{pmatrix} = \frac{1}{2} \begin{pmatrix} 1 + Z_{i+1}/Z_i & 1 - Z_{i+1}/Z_i \\ 1 - Z_{i+1}/Z_i & 1 + Z_{i+1}/Z_i \end{pmatrix} \begin{pmatrix} F_{il_i} \\ B_{il_i} \end{pmatrix}$$

together with

$$\begin{pmatrix} F_{il_i} \\ B_{il_i} \end{pmatrix} = \begin{pmatrix} e^{-sT_i} & 0 \\ 0 & e^{sT_i} \end{pmatrix} \begin{pmatrix} F_{i,0} \\ B_{i,0} \end{pmatrix}$$

This allows us to rewrite the expression as

$$\begin{pmatrix} F_{i+1,0} \\ B_{i+1,0} \end{pmatrix} = \frac{1}{2} \begin{pmatrix} (1+Z_{i+1}/Z_i)\, e^{-sT_i} & (1-Z_{i+1}/Z_i)e^{sT_i} \\ (1-Z_{i+1}/Z_i)e^{-sT_i} & (1+Z_{i+1}/Z_i)e^{sT_i} \end{pmatrix} \cdot \\ \cdot \begin{pmatrix} F_{i,0} \\ B_{i,0} \end{pmatrix}$$

We shall call the previous matrix T_{i+1}/i the *transmission matrix* for the $i : i+1$ interface:

$$\frac{T_{i+1}}{i} = \frac{1}{2} \begin{pmatrix} (1+Z_{i+1}/Z_i)\, e^{-sT_i} & (1-Z_{i+1}/Z_i)e^{sT_i} \\ (1-Z_{i+1}/Z_i)e^{-sT_i} & (1+Z_{i+1}/Z_i)e^{sT_i} \end{pmatrix}$$

Hence we can represent a multilayered structure using transmission matrices:

$$\frac{T_{n+1}}{1} = \frac{T_{n+1}}{n} \frac{T_n}{n-1} \cdots \frac{T_3}{2} \frac{T_2}{1}$$

where the matrix $T_{n+1}/1$ relates the force components $F_{(n+1)0}$ & $B_{(n+1)0}$ to F_{10} & B_{10}.

This can be expressed in matrix form as follows:

$$\begin{pmatrix} F_{(n+1)0} \\ B_{(n+1)0} \end{pmatrix} = \begin{pmatrix} T_{11} & T_{12} \\ T_{21} & T_{22} \end{pmatrix} \begin{pmatrix} F_{10} \\ B_{10} \end{pmatrix}$$

or

$$\begin{pmatrix} F_{(n+1)0} \\ B_{10} \end{pmatrix} = \begin{pmatrix} U_{11} & U_{12} \\ U_{21} & U_{22} \end{pmatrix} \begin{pmatrix} F_{10} \\ B_{(n+1)0} \end{pmatrix} = \\ = \begin{pmatrix} T_{11} - (T_{21}T_{12})/T_{22} & T_{12}/T_{22} \\ -T_{21}/T_{22} & 1/T_{22} \end{pmatrix} \begin{pmatrix} F_{10} \\ B_{(n+1)0} \end{pmatrix} \tag{27}$$

C. The multilayered transducer model

Now we shall put all the previous derivations together in the following setup, see figure 10.

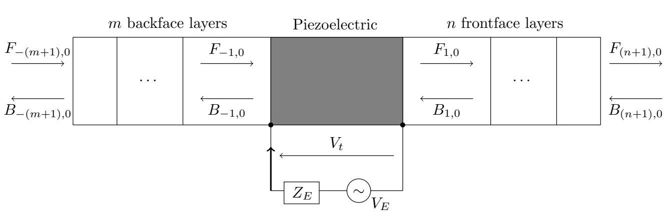

Fig. 10: The multilayer transducer model, putting all the previous situations together.

In this case, using (27) for the front and back faces:

$$\begin{pmatrix} F_{(n+1)0} \\ B_{10} \end{pmatrix} = \begin{pmatrix} U_{11}^F & U_{12}^F \\ U_{21}^F & U_{22}^F \end{pmatrix} \begin{pmatrix} F_{10} \\ B_{(n+1),0} \end{pmatrix}$$

$$\begin{pmatrix} B_{-(m+1)0} \\ F_{-10} \end{pmatrix} = \begin{pmatrix} U_{11}^B & U_{12}^B \\ U_{21}^B & U_{22}^B \end{pmatrix} \begin{pmatrix} B_{-10} \\ F_{-(m+1),0} \end{pmatrix}$$

what can be reexpressed as:

$$\boxed{\begin{pmatrix} F_{(n+1)0} \\ B_{-(m+1)0} \\ V_t \end{pmatrix} = \left(\mathbf{W_{ij}}\right) \begin{pmatrix} B_{(n+1),0} \\ F_{-(m+1),0} \\ V_E \end{pmatrix}}$$

where the coefficients are:

$$\begin{aligned}
W_{11} &= \{U_{21}^B(U_{11}^F U_{22}^F - U_{12}^F U_{21}^F)(P_{12}P_{21} - P_{11}P_{22}) + \\
&\quad + P_{11}U_{11}^F U_{22}^F + U_{12}^F(1 - P_{22}U_{21}^B - P_{11}U_{21}^F)\}/W_D \\
W_{12} &= U_{11}^F U_{22}^B P_{12}/W_D \\
W_{13} &= U_{11}^F \left\{U_{21}^B(P_{12}P_{33} - P_{13}P_{22}) + P_{13}\right\}/W_D \\
W_{21} &= U_{11}^B U_{22}^F P_{21}/W_D \\
W_{22} &= \{U_{21}^F(U_{11}^B U_{22}^B - U_{12}^B U_{21}^B)(P_{12}P_{21} - P_{11}P_{22}) + \\
&\quad + P_{22}U_{11}^B U_{22}^B + U_{12}^B(1 - P_{11}U_{21}^F - P_{22}U_{21}^B)\}/W_D \\
W_{23} &= U_{11}^B\{U_{21}^F(P_{21}P_{13} - P_{11}P_{23}) + P_{23}\}/W_D \\
W_{31} &= \left\{P_{31}U_{22}^F(1 - U_{21}^B P_{22}) + P_{31}U_{21}^B P_{21}U_{22}^F\right\}/W_D \\
W_{32} &= \left\{P_{32}U_{22}^B(1 - U_{21}^F P_{11}) + P_{32}U_{21}^F P_{12}U_{22}^B\right\}/W_D \\
W_{33} &= \{P_{33} + U_{21}^F(P_{31}P_{13} - P_{11}P_{33}) + U_{21}^B(P_{23}P_{32} - \\
&\quad - P_{22}P_{33}) + U_{21}^F U_{21}^B(P_{31}(P_{12}P_{23} - P_{13}P_{22}) + \\
&\quad + P_{32}(P_{21}P_{13} - P_{23}P_{11})P_{33}(P_{11}P_{22} - P_{12}P_{21}))\}/W_D
\end{aligned}$$

with $W_D = (1 - U_{21}^F P_{11})(1 - U_{21}^B P_{22}) - U_{21}^F U_{21}^B P_{12}P_{21}$.

We have then reduced all our multilayer system to a three inputs-outputs system. We can see that we recover the *receiver* and *transmitter* behaviour: for the receiver we will be interested in W_{31}, as we receive the input force $B_{(n+1),0}$ on the front face and all other inputs are set to zero. Similarly, for the transmitter we will look at W_{13}, as we assume no input forces and we drive our device applying a voltage V_E across its electrodes. Similarly, W_{33} relates the applied voltage to the voltage found across the transducer.

V. HUANG'S MODEL OF MULTILAYERED ULTRASONIC TRANSDUCERS, MODIFIED WITOUTH THE INVERSION LAYER

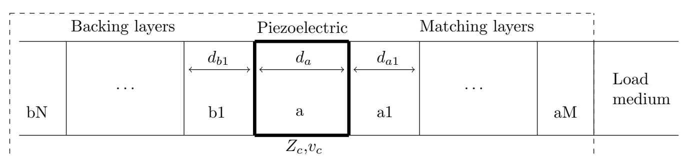

Fig. 11: Setup for an arbitrary number of pasive layers.

CONSIDER the multilayered setup detailed in figure 11. As explained in the introduction, this model uses a different framework, we no longer use Laplace transformed functions. Consider the interface between a and $b1$, keeping in mind that $b1$ is a passive layer and a is the active piezoelectric layer. The expressions for the particle velocities and pressures are:

At the left boundary of layer a:

$$\begin{cases} u_{a_{|LB}} = A_a e^{ik_a d_a/2} + B_a e^{-ik_a d_a/2} \\ p_{a_{|LB}} = z_a A_a e^{ik_a d_a/2} - z_a B_a e^{-ik_a d_a/2} + hD \end{cases}$$

At the right boundary of layer $b1$:

$$\begin{cases} u_{b1_{|RB}} = A_{b1} e^{-ik_{b1} d_{b1}/2} + B_{b1} e^{ik_{b1} d_{b1}/2} \\ p_{b1_{|RB}} = z_{b1} A_{b1} e^{-ik_{b1} d_{b1}/2} - z_{b1} B_{b1} e^{ik_{b1} d_{b1}/2} \end{cases}$$

And the boundary conditions impose that both velocities and pressures must be the equal:

$$\begin{cases} A_a e^{ik_a d_a/2} + B_a e^{-ik_a d_a/2} = \\ \qquad = A_{b1} e^{-ik_{b1} d_{b1}/2} + B_{b1} e^{ik_{b1} d_{b1}/2} & (28a) \\ z_a \left(A_a e^{ik_a d_a/2} - B_a e^{-ik_a d_a/2} \right) + hD = \\ = z_{b1} \left(A_{b1} e^{-ik_{b1} d_{b1}/2} - B_{b1} e^{ik_{b1} d_{b1}/2} \right) & (28b) \end{cases}$$

we will denote from now on $\alpha_j = k_j d_j$.

Now, the voltage across the only active layer of the transducer looks like

$$V = \int_{-d_a/2}^{d_a/2} E\, dx = -h \left(\xi_{d_a/2} - \xi_{-d_a/2} \right) + D/\varepsilon\, d_a = \\ = \frac{h}{i\omega} \left(e^{+i\alpha_a/2} - e^{-i\alpha_a/2} \right) (A_a - B_a) + D/\varepsilon\, d_a \tag{29}$$

and rearranging we can find the expression for D:

$$D = \frac{\varepsilon V}{d_a} - \frac{2h\varepsilon}{\omega d_a} \sin(\alpha_a/2) (A_a - B_a)$$

Thus, following Huang's calculations, we can now represent equations (28a) and (28b) in the following matrix form

$$\begin{pmatrix} 1 & 0 \\ 0 & z'_{b1} \end{pmatrix} \begin{pmatrix} \cos(-\alpha_{b1}/2) & i\sin(-\alpha_{b1}/2) \\ i\sin(-\alpha_{b1}/2) & \cos(-\alpha_{b1}/2) \end{pmatrix} \begin{pmatrix} H_{b1} \\ F_{b1} \end{pmatrix} = \\ = \begin{pmatrix} 1 & 0 \\ 0 & z'_a \end{pmatrix} \begin{pmatrix} \cos(-\alpha_a/2) & i\sin(-\alpha_a/2) \\ i\sin(-\alpha_a/2) & \cos(-\alpha_a/2) \end{pmatrix} \begin{pmatrix} H_a \\ F_a \end{pmatrix} + \\ + \begin{pmatrix} 0 \\ 1 - k_T^2 \mu_a F_a \end{pmatrix} \tag{30}$$

$$\text{where } k_T^2 = \frac{h^2 \epsilon}{Y}, \quad \mu_a = 2/\alpha_a \sin(\alpha_a/2),$$

$H_a = z_0 d_a / hV\epsilon (A_a + B_a)$ and $F_a = z_0 d_a / hV\epsilon (A_a - B_a)$

It is easy to check that we recover equations (28a) & (28b) if $z_0 = Y/v_a$. Rewrite now equation (30) as

$$\mathbf{M_{b1} G_{b1}^- x_{b1} = M_a G_a^+ x_a + s}$$

and repeating this calculations for all the interfaces we obtain

$$\begin{cases} M_{bN} \mathbf{G_{bN}^- x_{bN} = M_{b(N-1)} G_{b(N-1)}^+ x_{b(N-1)}} & (31a) \\ \vdots \mathbf{M_{b2} G_{b2}^- x_{b2} = M_{b1} G_{b1}^+ x_{b1}} & (31b) \\ \mathbf{M_{b1} G_{b1}^- x_{b1} = M_a G_a^+ x_a + s} & (31c) \\ \mathbf{M_a G_a^- x_a + s = M_{a1} G_{a1}^+ x_{a1}} & (31d) \\ \vdots \mathbf{M_{a(M-1)} G_{a(M-1)}^- x_{a(M-1)} = M_{aM} G_{aM}^+ x_{aM}} & (31e) \end{cases}$$

which are $2{\cdot}(N{+}M)$ linear equations, and $\mathbf{G_{bN}^-} = \mathbf{G_{aM}^+} = \mathrm{Id}$ & $A_{bN} = B_{aM} = 0$.

In the very front and back layers there is no incoming and returning wave (respectively), this is $A_{bN} = B_{aM} = 0$, resulting in:

$$x_{aM} = \begin{pmatrix} H_{aM} \\ F_{aM} \end{pmatrix} = \begin{pmatrix} A_{aM} \dfrac{z_0 d}{\epsilon h V} \\ A_{aM} \dfrac{z_0 d}{\epsilon h V} \end{pmatrix} = \begin{pmatrix} A'_{aM} \\ A'_{aM} \end{pmatrix}$$

$$x_{bN} = \begin{pmatrix} H_{bN} \\ F_{bN} \end{pmatrix} = \begin{pmatrix} B_{bN} \dfrac{z_0 d}{\epsilon h V} \\ -B_{bN} \dfrac{z_0 d}{\epsilon h V} \end{pmatrix} = \begin{pmatrix} B'_{bN} \\ -B'_{bN} \end{pmatrix}$$

Due to the form of the equations, we can now reduce them using transmission matrices, the procedure is detailed below. We shall start with the front layers: consider first equation (31d):

$$\mathbf{M_a G_a^- x_a + s = M_{a1} G_{a1}^+ x_{a1}}$$

from the next equation we can write

$$\mathbf{x_{a1}} = (\mathbf{M_{a1} G_{a1}^-})^{-1} (\mathbf{M_{a2} G_{a2}^+}) \mathbf{x_{a2}}$$

Similarly, from the following one

$$\mathbf{x_{a2}} = (\mathbf{M_{a2} G_{a2}^-})^{-1} (\mathbf{M_{a3} G_{a3}^+}) \mathbf{x_{a3}}$$

and so on. Substituting the obtained expressions we get to:

$$\mathbf{M_a G_a^- x_a + s = M_{a1} G_{a1}^+} [(\mathbf{M_{a1} G_{a1}^-})^{\mathbf{-1}} (\mathbf{M_{a2} G_{a2}^+})] \cdot \\ \cdot [(\mathbf{M_{a2} G_{a2}^-})^{\mathbf{-1}} (\mathbf{M_{a3} G_{a3}^+})] \ldots [(\mathbf{M_{a(M-1)} G_{a(M-1)}^-})^{\mathbf{-1}} \cdot \\ \cdot (\mathbf{M_{aM} G_{aM}^+})] \mathbf{x_{aM}} = [(\mathbf{M_{a1} G_{a1}^+})(\mathbf{M_{a1} G_{a1}^-})^{\mathbf{-1}}] \cdot \\ \cdot [(\mathbf{M_{a2} G_{a2}^+})(\mathbf{M_{a2} G_{a2}^-})^{\mathbf{-1}}] \ldots [(\mathbf{M_{a(M-1)} G_{a(M-1)}^+}) \\ (\mathbf{M_{a(M-1)} G_{a(M-1)}^-})^{\mathbf{-1}}] \mathbf{M_{aM} G_{aM}^+ x_{aM}} = \\ (\mathbf{T_{a1}^+ \ldots T_{a(M-1)}^+}) \mathbf{M_{aM} G_{aM}^+ x_{aM}} = \\ = \mathbf{T_a^+ M_{aM} G_{aM}^+ x_{aM} = M_a G_a^+ x_a + s}$$

where $\mathbf{T_a^+}$ is the *transmission matrix* from the front layer to the transducer front face. Each of the single transmission matrices is as follows

$$\mathbf{T_{am}^+ = M_{am} G_{am}^+ \left(M_{am} G_{am}^- \right)^{-1}} = \\ \begin{pmatrix} 1 & 0 \\ 0 & z'_{am} \end{pmatrix} \cdot \begin{pmatrix} \cos(\alpha_m/2) & i\sin(\alpha_m/2) \\ i\sin(\alpha_m/2) & \cos(\alpha_m/2) \end{pmatrix} \cdot \\ \cdot \begin{pmatrix} \cos(-\alpha_m/2) & i\sin(-\alpha_m/2) \\ i\sin(-\alpha_m/2) & \cos(-\alpha_m/2) \end{pmatrix}^{-1} \begin{pmatrix} 1 & 0 \\ 0 & z'_{am} \end{pmatrix}^{-1} = \\ = \begin{pmatrix} \cos^2(\alpha_m/2) - \sin^2(-\alpha_m/2) & 2i/z'_{am} \cos(\alpha_m/2)\sin(\alpha_m/2) \\ 2iz'_{am} \cos(\alpha_m/2)\sin(\alpha_m/2) & \cos^2(\alpha_m/2) - \sin^2(-\alpha_m/2) \end{pmatrix} = \\ = \begin{pmatrix} \cos(\alpha_m/2) & i/z'_{am} \sin(\alpha_m/2) \\ i/z'_{am} \sin(\alpha_m/2) & \cos(\alpha_m/2) \end{pmatrix} \tag{32}$$

where we have used the following trigonometric identities $\cos^2 x - \sin^2 x = \cos(2x)$ and $\sin x \cos x = \sin(2x)/2$.

We can perform the same calculations for the backing layers, starting with (31c)

$$\mathbf{M_{b1} G_{b1}^- x_{b1} = M_a G_a^+ x_a + s}$$

from the previous equation we can write

$$\mathbf{x_{b1}} = (\mathbf{M_{b1}G^+_{b1}})^{-1}(\mathbf{M_{b2}G^-_{b2}})\mathbf{x_{b2}}$$

Similarly, from the previous one

$$\mathbf{x_{b2}} = (\mathbf{M_{b2}G^+_{b2}})^{-1}(\mathbf{M_{b3}G^-_{b3}})\mathbf{x_{b3}}$$

and so on. Substituting the obtained expressions we get to:

$$\begin{aligned}
&\mathbf{M_aG^+_ax_a} + \mathbf{s} = \mathbf{M_{b1}G^-_{b1}}[(\mathbf{M_{b1}G^+_{b1}})^{-1}(\mathbf{M_{b2}G^-_{b2}})]\cdot \\
&\cdot[(\mathbf{M_{b2}G^+_{b2}})^{-1}(\mathbf{M_{b3}G^-_{b3}})]\dots[(\mathbf{M_{b(N-1)}G^+_{b(N-1)}})^{-1}\cdot \\
&\cdot(\mathbf{M_{bN}G^-_{bN}})]\cdot\mathbf{x_{bN}} = [\mathbf{M_{b1}G^-_{b1}}(\mathbf{M_{b1}G^+_{b1}})^{-1}]\cdot \\
&\cdot[\mathbf{M_{b2}G^-_{b2}}(\mathbf{M_{b2}G^+_{b2}})^{-1}]\dots[(\mathbf{M_{b(N-1)}G^-_{b(N-1)}}) \\
&(\mathbf{M_{b(N-1)}G^+_{b(N-1)}})^{-1}]\mathbf{M_{bN}G^-_{bN}x_{bN}} = \\
&= (\mathbf{T^-_{b1}}\dots\mathbf{T^-_{b(N-1)}})\mathbf{M_{bN}G^-_{bN}x_{bN}} = \\
&= \mathbf{T^+_bM_{bN}G^-_{bN}x_{bN}} = \mathbf{M_aG^+_ax_a} + \mathbf{s}
\end{aligned}$$

where $\mathbf{T^-_{bn}}$ is the *transmission matrix* from the back layer to the transducer rear face. Each of the single transmission matrices is as follows, in a completely analogous fashion as we did before:

$$\begin{aligned}
\mathbf{T^-_b} &= (\mathbf{M_{bn}G^-_{bn}})(\mathbf{M_{bn}G^+_{bn}})^{-1} = \\
&= \begin{pmatrix} \cos(-\alpha_n/2) & i/z'_{an}\sin(-\alpha_n/2) \\ i/z'_{an}\sin(-\alpha_n/2) & \cos(-\alpha_n/2)\end{pmatrix}
\end{aligned} \tag{33}$$

Using (32) and (33) we can rewrite equations (31a)-(31e) in the more compact matrix form

$$\begin{cases} \mathbf{T^-_bM_{bN}G^-_{bN}x_{bN}} = \mathbf{M_aG^+_ax_a} + \mathbf{s} \\ \mathbf{M_aG^-_ax_a} + \mathbf{s} = \mathbf{T^+_aM_{aM}G^+_{aM}x_{aM}} \end{cases}$$

but M_a, G^+_{aM} and G^-_{bN} can be set to the identity matrix, yielding to

$$\begin{cases} \mathbf{T^-_bM_{bN}x_{bN}} = \mathbf{G^+_ax_a} + \mathbf{s} \\ \mathbf{G^-_ax_a} + \mathbf{s} = \mathbf{T^+_aM_{aM}x_{aM}} \end{cases} \tag{34}$$

where

$$x_{aM} = \begin{pmatrix} A'_{aM} \\ A'_{aM} \end{pmatrix} \ \ \& \ \ x_{bN} = \begin{pmatrix} B'_{bN} \\ -B'_{bN} \end{pmatrix}$$

As a last step, we can write (34) as a single linear system $Ax = b$. From (34) we obtain:

$$\begin{cases}
-a_{32}B'_{bN} - [\cos(\alpha_a/2)H_a + i\sin(\alpha_a/2)F_a] - 0 = 0 \\
-a_{42}B'_{bN} - [i\sin(\alpha_a/2)H_a + \cos(\alpha_a/2)F_a] - \\
\qquad\qquad - \left[1 - k_T^2\mu_aF_a\right] = 0 \\
a_{11}A'_{aM} - [\cos(-\alpha_a/2)H_a + i\sin(-\alpha_a/2)F_a] - 0 = 0 \\
-a_{21}A'_{aM} - [i\sin(-\alpha_a/2)H_a + \cos(-\alpha_a/2)F_a] - \\
\qquad\qquad - \left[1 - k_T^2\mu_aF_a\right] = 0
\end{cases}$$

where

$$a_{11} = [T^+_a(1,1) + T^+_a(1,2)z'_{aM}]$$

$$a_{21} = [T^+_a(2,1) + T^+_a(2,2)z'_{aM}]$$

$$a_{32} = -[T^-_b(1,1) + T^-_b(1,2)z'_{bN}]$$

$$a_{42} = -[T^-_b(2,) + T^+_a(2,2)z'_{bN}]$$

Thus we can finally write

$$\boxed{\begin{pmatrix} a_{11} & 0 & -c^-_a & -is^-_a \\ a_{21} & 0 & -is^-_a & -c^+_a + k_T^2\mu_a \\ 0 & a_{32} & c^+_a & is^+_a \\ 0 & a_{42} & is^+_a & c^+_a - k_T^2\mu_a \end{pmatrix} \cdot \begin{pmatrix} A'_{aM} \\ B'_{bN} \\ H_a \\ F_a \end{pmatrix} = \begin{pmatrix} 0 \\ 1 \\ 0 \\ 1 \end{pmatrix}}$$

where $c^\pm_a = \cos(\pm\alpha_a/2)$ and $s^\pm_a = \sin(\pm\alpha_a/2)$.

We can easily solve this system using for example Cramer's rule.

To finish with this model, we can write the expression for the transducer impedance as follows: consider equation (29)

$$\begin{aligned}
&V = \frac{h}{i\omega}\left(e^{+i\alpha_a/2} - e^{-i\alpha_a/2}\right)(A_a - B_a) + D/\varepsilon\, d_a \Longrightarrow \\
&\Longrightarrow \frac{Dd_a}{\varepsilon} = V\left[1 - \frac{h^2\varepsilon}{Y}\frac{2}{\alpha_a}\sin(\alpha_a/2)\frac{z_od_a}{hV\varepsilon}(A_a - B_a)\right] \\
&\Longrightarrow \frac{Dd_a}{\varepsilon} = V\left[1 - k_T^2\mu_aF_a\right] \Longrightarrow D = \frac{\varepsilon V}{d_a}\left[1 - k_T^2\mu_aF_a\right]
\end{aligned}$$

thus the electrical current through the transducer is

$$I = i\omega DS = i\omega S\frac{\varepsilon V}{d_a}(1 - k_T^2\mu_aF_a) = i\omega C_o(1 - k_T^2\mu_aF_a)V$$

and the impedance

$$\boxed{Z = \frac{V}{I} = \frac{1}{i\omega C_o}\frac{1}{1 - k_T^2\mu_aF_a}} \tag{35}$$

VI. Analytical results

IN the three previous sections we have introduced and defined three different analytical models that varied in capabilities and modelling techniques. For a considered transducer, all will provide analyical results for the *transmitter* and *receiver* force-voltage relations and the *electrical impedance* behaviour.

To test our models against *FEM* and real data from the laboratory, we have considered three test cases whose specifications can be found in the following table:

	Test Case 1	Test Case 2	Test Case 3
Material	PZT	PZT	PZT
Dim	25x25mm	20x20mm	20x20mm
Thickness	0.5mm	1mm	2mm

The three transducers are made of Lead zirconate titanate (PZT), one of the most common piezoelectric materials. Notice the lateral dimensions-thickness ratio for the three of them, beginning with a reasonably high value and decreasing afterwards. As the considered analytical models are 1D, we will check how well this approximation holds for real world devices.

A. *Transducer impedance*

The results for the impedance modulus are shown in figures 12,13 & 14. The spike on the right hand side of the plot corresponds to the main resonance region, while the descending curve on the left hand side corresponds to the lateral resonance behaviour.

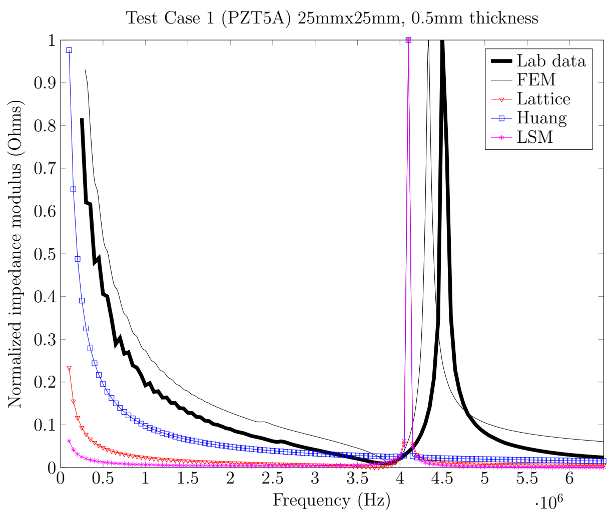

Fig. 12: Electrical impedance modulus for test case 1

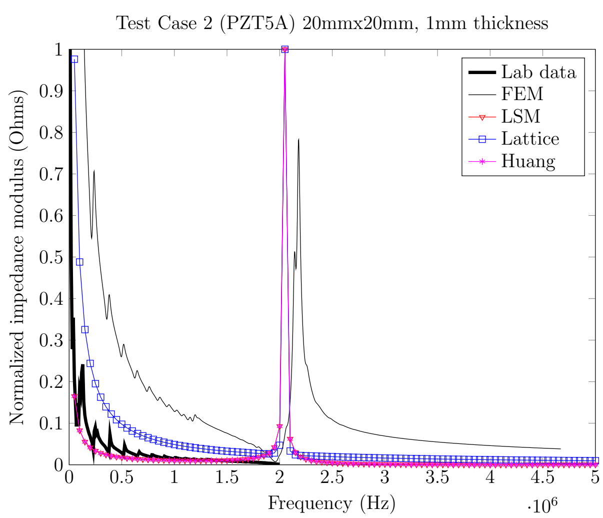

Fig. 13: Electrical impedance modulus for test case 2

We can see good agreement with the real data for the three cases, although the *FE* model's predictions are closer to reality. Due to the lack of lateral dimensions and any kind of attenuation or loss mechanism we can see our models predicting a narrower and earlier peak. Due to a laboratory problem, the data for the second test case is incomplete, but we can still appreciate its behaviour. All the plots are normalized to the unit due to some magnitude discordances among the models.

It is not shown in the pictures for the sake clarity, but we are also able to predict the impedance peak's harmonics in

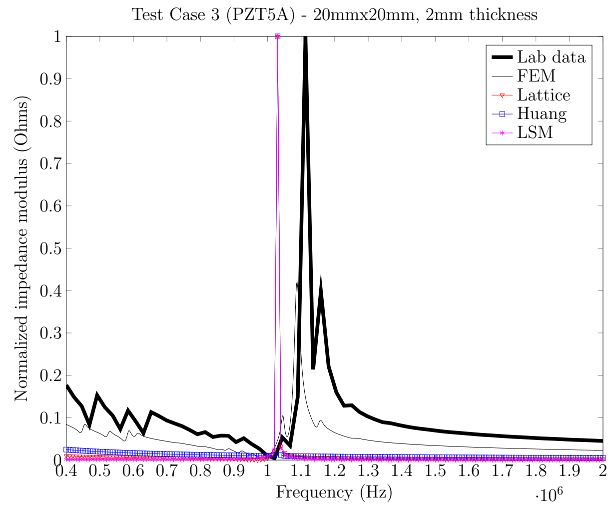

Fig. 14: Electrical impedance modulus for test case 3

higher frequencies, agreeing as well with the laboratory data.

Similarly, we show below the results for the impedance phase (figures 15, 16 & 17), we can see good agreement predicting the peak area.

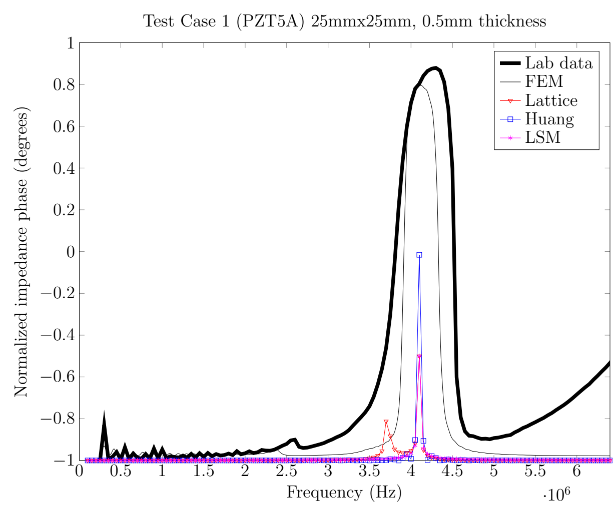

Fig. 15: Electrical impedance phase for test case 1

We have then tested some realistic devices and found that we can successfully predict their behaviour in a fast and clean way using analytical models. Let's see now how to interpret the impedance results: when designing or analyzing a given transducer, we want to locate its impedance peaks, which will be the desired operating frequencies, as we will get the best behaviour there. This is then the first step in the design process.

B. *Transducer bandwidth*

We will define *bandwidth* as the range of frequencies for which the signal power has dropped to half of its maximum value (-3 dB). In the case of ultrasonic transducers, the signal will be the force output when transmitting and the voltage output when receiving (completely analogous results using

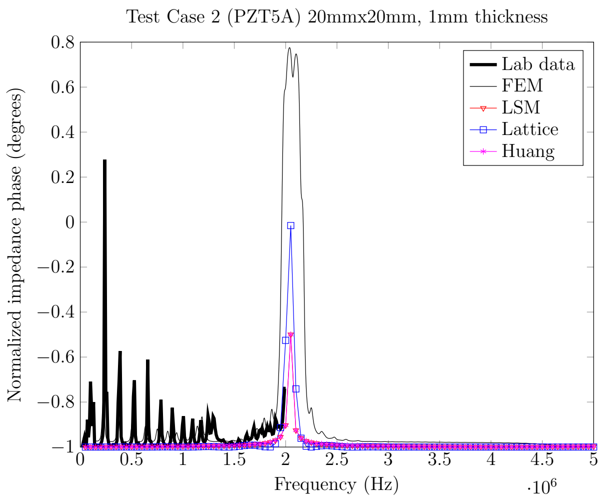

Fig. 16: Electrical impedance phase for test case 2

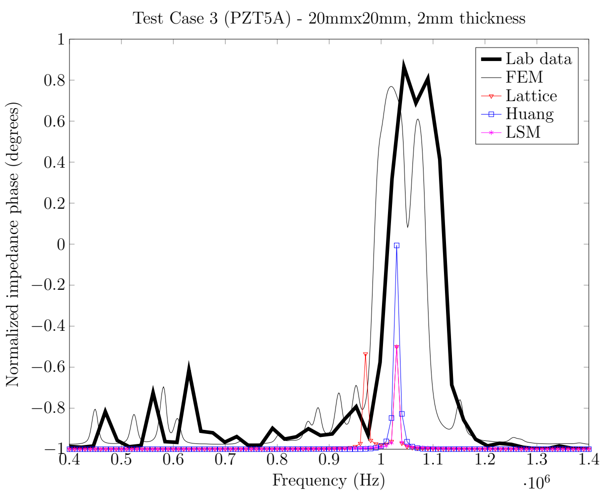

Fig. 17: Electrical impedance phase for test case 3

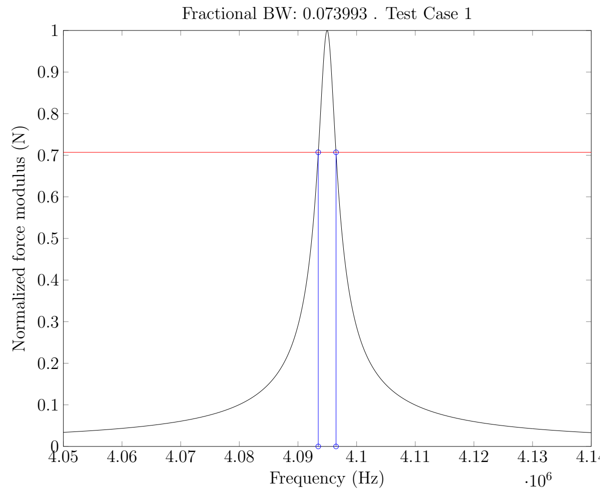

Fig. 18: Fractional bandwidth for test case 1

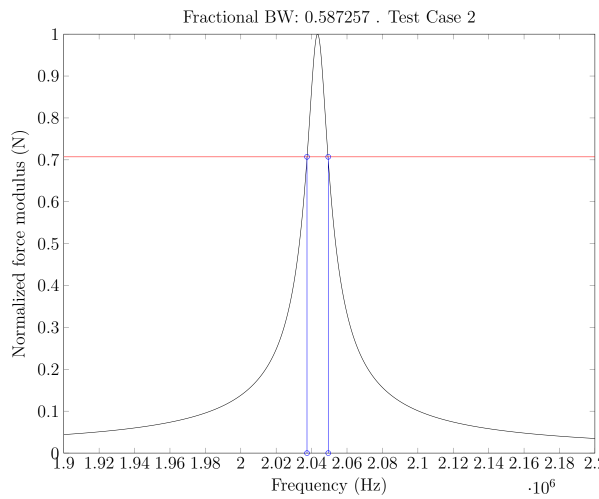

Fig. 19: Fractional bandwidth for test case 2

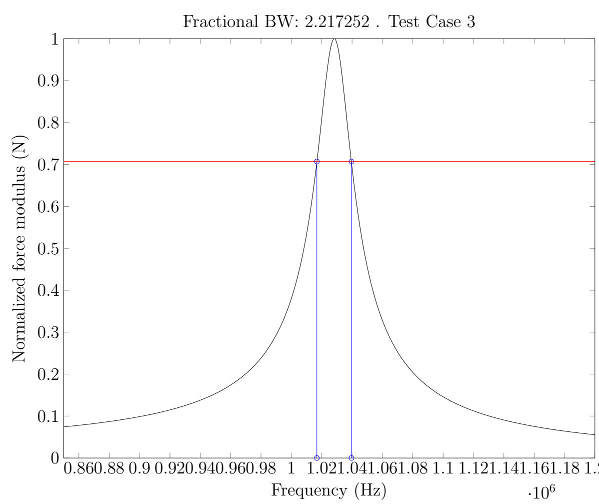

Fig. 20: Fractional bandwidth for test case 3

either of them). Similarly, the *fractional bandwidth* is defined as bandwidth divided by the maximum frequency. Higher bandwidth means a wider curve and smaller bandwidth a narrower one. We will want to design our transducers so that they get higher fractional bandwidth as possible, so that we can efficiently operate the device in a wider range of frequencies. In time domain this is equivalent to short ringing signal and consequently better response.

Our results for the three transducers are presented below (figures 18,19 & 20). The obtained fractional bandwidth is probably not very accurate as our analytical models predict narrower peaks, but as we will see later it still provides good qualitative behaviour.

A mismatch between transducer and loading medium acoustic impedances will result in poor bandwidth and energy transfer, being them increased as both impedances get closer. Hence, a preliminary test for our models will consist of varying the theoretical loading medium impedance and find the maximum in the fractional bandwidth curve, which is shown below (figure 21).

The black vertical line shows the transducer impedance, ideally we should get the maximum exactly at that point, but due to the tendency of finding the maximum impedance peaks a bit shifted, we find a maximum point which is close to the theoretical result. The third test case, the one further from 1D approximation, presents some drift for higher impedances.

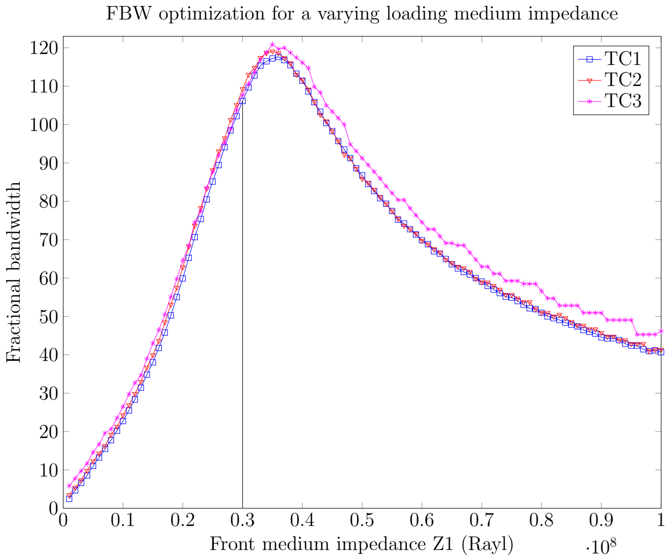

Fig. 21: Acoustical impedance optimization

C. Bandwidth and matching layers

When designing an application specific transducer with a given loading medium, the matching layers come into play: their purpose it to minimize the acoustic impedance mismatch between the transducer and the loading medium.

Literature gives the ideal impedance value for a single matching layer as the geometric mean of the transducer and loading medium impedances: $Z = \sqrt{Z_t Z_l}$. The other important aspect of the matching layers is their thickness: optimal thickness for a single matching layer is a quarter of the operating wavelength ($\lambda = c/f$, being c the speed of sound in the selected material and f the frequency). When the thickness of the piezoelectric layer is $\lambda/2$ this guarantees that waves that are reflected within the matching layer are in phase when exiting the layer, hence maximum energy transmission is achieved. [7]

We have tested this results analytically using *lattice model*, the results plotted below: we have considered a single matching layer with optimum impdance, and different thicknesses varying from zero to twice the thickness of the piezoelectric layer. The first dashed line corresponds to $\lambda/4$ thickness, and the gap between any two consecutive lines is $\lambda/2$, this will also keep reflected waves in phase. It is worth mentioning that our piezoelectric thicknesses are way larger than the optimum $\lambda/2$ explained before, so we may see discrepances with the optimum matching thickness as well.

We can see very good agreement in the two first test cases: higher bandwidth is obtained as predicted theoretically. For the first one, the model predicts as well high bandwidth peaks at the successive $\lambda/2$ jumps. The second one seems to have destructive wave interaction for early jumps, being maybe stabilized at a later stage. However it is difficult to judge because the dashed lines cut the bandwidth curve at very steep points. The third case is more difficult to interpret: we definitely see the spike behaviour located around the dashed lines, but it does not agree with the expected behaviour. This may be caused by numerical instabilities or by a too small lateral dimensions-thickness ratio, making theh 1D model insuficient for this kind of analysis. In this case, further analysis using laboratory instrumentation or *FEM* should be used.

Summarizing, nice agreement with theory is found using the two first test cases, while the third one needs further testing. It seems to work fine for transducers thoroughly satisfying our assumptions. Deeper and broader analysis must be performed for other transducers to check the validity of this models.

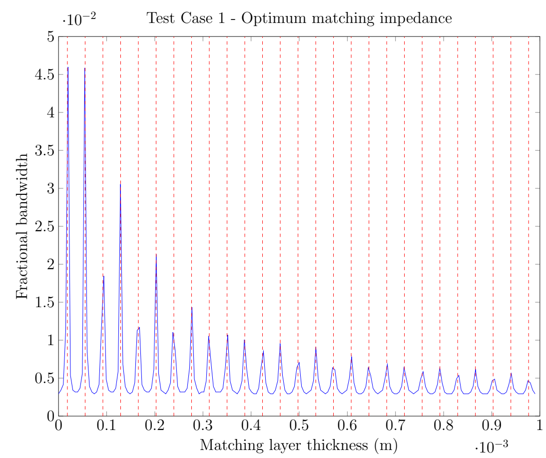

Fig. 22: Matching layer optimization for TC1

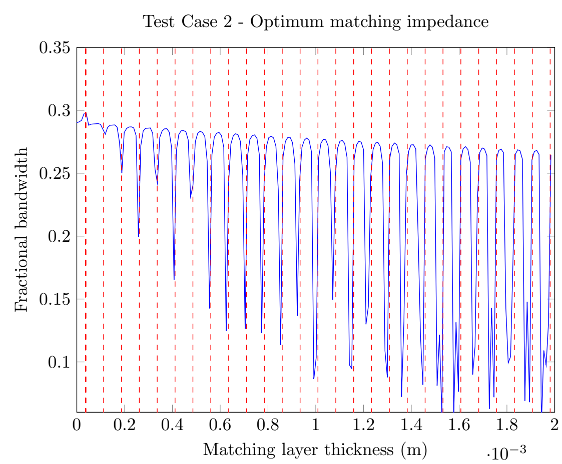

Fig. 23: Matching layer optimization for TC2

D. Communication systems: pitch-catch

As a last setup for our models we will consider simulating a complete transducer system, that is typically seen in practical

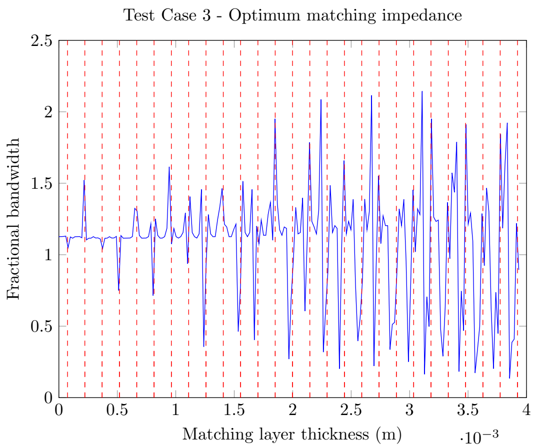

Fig. 24: Matching layer optimization for TC3

applications: we place two ultrasonic transducers at both sides of an in-between medium, this can be a wall or other kind of object (see figure 18).

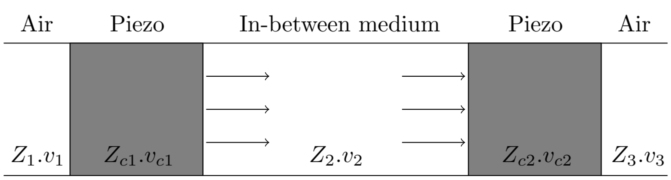

Fig. 25: Pitch-catch transmission system

One of them will act as a transmitter and the other one will receive the transmitted wave. This kind of systems have started being used in places where conventional wired communication is not possible, for example in submarines or in any kind of pressurized enclosure. This kind of ultrasonic communication problem is usually approached using an ad-hoc procedure, get the transducers in place and test them using a short pulse trying to obtain the frequency signature that would be used to model more complex waves.

Hence we can try to apply analytical modelling to this problem: we shall use the *linear systems model* for both transmitter and receiver. To use this model we have to assume that the in-between medium's thickness is much larger that the transducer, this shoud not be a problem though. We will hit the transmitter with an ideal pulse and obtain the force output in frequency domain, finally we will plug it into the receiver, obtaining the final voltage output. We could use an *inverse Fourier transform* to get the time domain respresentation and then use convolution to obtain the final output.

The analytical model gives the following: applying a voltage e to the transmitter, the transfer function for the output force is, using equation (17)

$$F_{F1} = -\frac{e \cdot h \cdot a(s) Z_2/(Z_{c1} + Z_2)\, K_{F1}(s) Y(s)}{1 - h^2 Y(s)/(sZ_c)\,(T_{F1}K_{F1}/2 + T_{B1}K_{B1}/2)}$$

where the coefficients are detailed in the third section, considering the new index notation specified in the figure.

Then, for the receiver, using (12)

$$V = \frac{-F \cdot h \cdot K_{F2}T_{F2}U(s)/sZ_{c2}}{1 - h^2\left[\frac{K_{F2}T_{F2}}{2} + \frac{K_{B2}T_{B2}}{2}\right]\frac{U(s)}{s^2 Z_e Z_{c2}}} =$$
$$= \frac{h \cdot K_{F2}T_{F2}U(s)/sZ_{c2}}{1 - h^2\left[\frac{K_{F2}T_{F2}}{2} + \frac{K_{B2}T_{B2}}{2}\right]\frac{U(s)}{s^2 Z_e Z_{c2}}} \cdot$$
$$\cdot \frac{e \cdot h \cdot a(s) Z_2/(Z_{c1} + Z_2)\, K_{F1}(s) Y(s)}{1 - h^2 Y(s)/(sZ_c)\,(T_{F1}K_{F1}/2 + T_{B1}K_{B1}/2)}$$

To test the results we have used the first test case transducer as transmitter and receiver. The in-between medium is chosen to be *steel* ($Z_2 = 45$MRayl) with large enough thickness. The results are presented below.

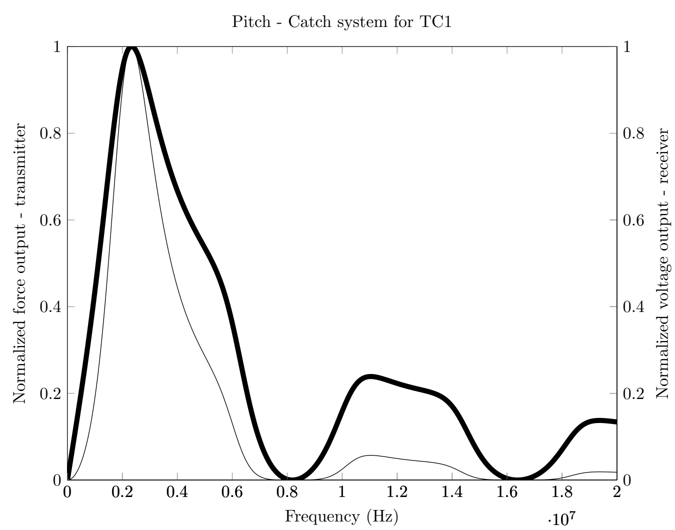

Fig. 26: Pitch-catch transmission system i/o using TC1

The thick curve is the generated force in the transmitter, and the thin one is the generated voltage in the receiver. We can see that we receive a similar but attenuated signal. Similar results are obtained using the other two test cases. The system can be improved introducing matching layers and chosing a better backing than air. It would also be interesting to obtain an analytical model comprising both transmitter and receiver in a compact way, *i.e.* solve the wave equations for the present boundary conditions (see figure 10).

VII. Conclusions

WE have explained and tested three different analytical models for ultrasonic transducers in a variety of experiments to check their behaviour, obtaining typically good results, although when the transducer gets a bit far from the models' assumptions, predictions break and one has to be more careful.

Our models allow us to find the optimal operating frequencies for each considered transducer. Once this is achieved, our interest will be maximizing the bandwidth and the energy transmission. This will be done using matching layers, whose optimum impedance and thickness can be obtained analytically.

Thus analytical models are a good tool for design and optimization purposes, providing an insight into the undelying physics. This kind of models are also very fast and can be easily coded, in contraposition with *FE* models which are much slower and computationally expensive, and usually come in the form of commercial software packages.

VIII. Acknowledgement

I would like to thank Nishal Ramadas for all the help and training provided.

References

[1] M. Willatzen, *Ultrasound transducer modelling – general theory and applications to ultrasound reciprocal systems*, IEEE Transactions on Ultrasonics, Ferroelectrics and Frequency Control, vol. 48, No 1, January 2001.

[2] M. Redwood, *Transient performance of a piezoelectric trasnducer*, J. Acoust. Soc. Am. **33** (4), April 1961.

[3] G. Hayward, C. J. MacLeod, *A systems model of the thickness mode piezoelectric transducer*, J. Acoust. Soc. Am. **76** (2), August 1984.

[4] N. Ramadas, G. Hayward, C. J. C. Barbenel, Y. Estanbouli, *A linear systems model of the thickness mode piezoelectric transducer containing dual piezoelectric zones* , Ultrasonics Symposium, 2004 IEEE, Vol. 3.

[5] G. Hayward, M. N. Jackson, *A lalttice model of the thickness-mode piezoelectric transducer*, IEEE Transactions on Ultrasonics, Ferroelectrics and Frequency Control, vol. UFFC-33, No 1, January 1986.

[6] C Huang, M. V. Z. Marmarelis, Q. Zhou, K. K. Shung *An analytical model of multilayer ultrasonic transducers with an inversion layer*, IEEE Transactions on Ultrasonics, Ferroelectrics and Frequency Control, vol.52, No 3, March 2005.

[7] T. E. Gómez Álvarez-Arenas and Luis Díez, *Novel impedance matching materials and strategies for air-coupled piezoelectric transducers*, SENSORS, 2013 IEEE Conference, November 2013.